DOI: 10.1002/ejic.200601169

Ligand Exchange Processes on Solvated Lithium Cations: Complexation by Cryptands in Acetone as Solvent[‡]

Ewa Pasgreta,[a] Ralph Puchta,[a,b] Achim Zahl,[a] and Rudi van Eldik*[a]

Keywords: Lithium / Cryptands / Acetone / Exchange mechanism

Kinetic studies on Li^+ exchange between the cryptands C222 and C221 and acetone as solvent were performed as a function of ligand-to-metal ratio, temperature and pressure using ^7Li NMR spectroscopy. Temperature and pressure dependence measurements were performed in the presence of an excess of Li^+. The rate and activation parameters for the exchange process are: C222: $k_{298} = (1.7 \pm 0.5) \times 10^3$ s^{-1}, $\Delta H^{\#} = 24 \pm 1$ $kJ\,mol^{-1}$ and $\Delta S^{\#} = -105 \pm 4$ $J\,K^{-1}\,mol^{-1}$; C221: $k_{298} = 2.24 \pm 0.09$ s^{-1}, $\Delta H^{\#} = 29 \pm 2$ $kJ\,mol^{-1}$ and $\Delta S^{\#} = -141 \pm 5$ $J\,K^{-1}\,mol^{-1}$. The influence of pressure on the exchange rate is insignificant for both ligands, such that the activation volume is around zero within the experimental error limits. The reported activation parameters suggest that the exchange of Li^+ between solvated and chelated ions follows an associative interchange mechanism.

Introduction

Following the work of Pedersen on two-dimensional crowns, Lehn and co-workers developed in the late 1960s a range of three-dimensional, polycyclic ligand systems which they named cryptands (Greek: *cryptos* = cave).[1] Until today this class of compounds has been intensively explored and extended in different directions[2] in terms of cavity size,[3,4] donor atoms,[5] and metalla-topomers.[6] Because cryptands readily form complexes with a wide range of metal ions and NH_4^+,[7] provided the ion involved is not too large to be contained in the macrocyclic cavity,[8] they find their application in various areas like catalysis, medicine, biomimetic research,[9,10] and as receptors[11] and electrides.[12] Studies on the complexes (cryptates) formed between alkali-metal ions and cryptands, have revealed a substantial understanding of the effects of metal-ion size and cryptand-cavity size on the structure, stability and lability of cryptates, and the mechanism of the cryptate complex-formation processes.[13,14] Such selective complexation has led to many biological and chemical studies.

Kinetic studies on macrocyclic complex-formation reactions with alkali cations not only result in important information on the rates and mechanisms of complex-formation reactions, but also lead to a better understanding of the high selectivity of these ligands toward different cations. The broad impact of such studies spans from the theory of complexation to cation transport through membranes, and makes the ability to control cation selectivity via tactical structural changes in the complexing agent of prime importance.[10] Polyoxo macrobicyclic diamines, represented by the structure in Figure 1, are able to form metal-ion complexes in which the metal ion is located in the cavity of the macromolecule and two nitrogen donors along with the oxygen donors participate in binding the metal cation. All complexes have a 1:1 stoichiometry with the metal ion positioned at the center of the ligand cavity.[13]

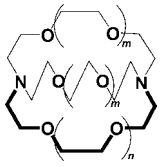

Figure 1. Chelate structures: C211: $m = 0$, $n = 1$; C221: $m = 1$, $n = 0$; C222: $m = 1$, $n = 1$.

In case of crown ethers and cryptands in non-aqueous solutions, the rates of complex-formation (k_f) with alkali-metal cations are in general diffusion-controlled and, consequently, the complexation selectivities are governed by the decomplexation rates (k_d).[15] These reactions have received significant attention, initially from Lehn and co-workers and more recently from Popov et al.[16,17] and Lincoln et al.[18] Many examples have been included in a series of review articles.[19,20] It has been reported that ligand structure and solvent properties have considerable effects on the reaction rates, activation parameters, and exchange mechanism

[‡] Part V. Part IV: E. Pasgreta, R. Puchta, A. Zahl, R. van Eldik, *Eur. J. Inorg. Chem.*, in press.

[a] Institute for Inorganic Chemistry, University of Erlangen-Nürnberg,
Egerlandstr. 1, 91058 Erlangen, Germany
E-mail: vaneldik@chemie.uni-erlangen.de
[b] Computer Chemistry Center, University of Erlangen-Nürnberg, Nägelsbachstr. 25, 91052 Erlangen, Germany

Supporting information for this article is available on the WWW under http://www.eurjic.org or from the author.

of cations between the solvated and complexed sites. We have now extended our earlier studies[21] on Li^+ exchange reactions to acetone as solvent.

Non-aqueous solvents and their mixtures combined with Li^+ are often used in secondary lithium batteries.[22] Li^+ in acetone is also known to catalyze Diels–Alder-reactions[23] and the ene reaction.[24] The behavior of Li^+-ions in different solvents is therefore an important research area.[25–27] A variety of studies on solutions of Li^+ in acetone have been mainly studied experimentally[26,28] and some theoretically,[29,30] as well as for solvent/acetone combinations[27] or chelator/acetone combinations.[27,31] In this contribution, we focus on acetone as a solvent and the competition between solvated and endohedral complexed Li^+, report kinetic parameters for the exchange of Li^+ between solvated and complexed states in acetone under ambient and elevated pressure conditions, and discuss the mechanistic implications.

Results and Discussion

Spectroscopic and Kinetic Observations

In preliminary experiments we investigated the Li^+ exchange in different solvents. In water and methanol the exchange process was too fast to be studied by ^7Li NMR (only a single signal was observed). The process became slower in acetonitrile, and in acetone two completely separated signals were observed at low temperature. We, therefore, investigated Li^+ exchange between the selected cryptands and acetone as solvent. A similar system was also investigated before by Popov et al.[17] Although they reported a significantly negative value for the activation entropy, they suggested the operation of a dissociative exchange mechanism. We realized that it would be worth to perform a reinvestigation of this system in acetone in order to clarify this apparent discrepancy, in particular by means of high pressure ^7Li NMR spectroscopy.

Initially, a series of ^7Li NMR measurements for the Li^+–cryptand system in acetone were performed. For each of the cryptands C222, C221 and C211, molar ratio dependent measurements were performed by variation of both the cryptand/Li^+ and Li^+/cryptand molar ratios. The results enabled us to observe the distribution of particular species on variation of the concentration ratio. Basically, two signals of varying intensity were observed in the ^7Li NMR spectra that refer to solvated Li^+ and Li^+ bound inside the cryptand cavity. In case of the smallest chelate C211, however, an additional signal appeared which can be ascribed to Li^+ bound outside the cryptand and being partially solvated. In the case of $Li(C211)^+$, the complex is very stable and almost no exchange takes place. A detailed study of the observed rate constant, $k_{obsd.}$, for the exchange of Li^+ as a function of temperature and pressure was therefore undertaken only for C221 and C222. The lithium exchange reaction between cryptand and acetone was studied for three solutions with different ligand-to-metal ratios in the presence of an excess of Li^+.

Three signals can be observed in Figure 2, viz. one coming from the reference (δ = 5.8 ppm) and the other two from the exchanging sites (δ = 9.0 ppm for solvated Li^+ and 6.6 ppm for complexed Li^+). At low temperature the signals are sharp and completely separated due to very slow or no exchange. Because the formation constant for $Li(C221)^+$ is very high,[13] the concentration of bound lithium equals the amount of cryptand added. At ca. 283 K, the signals start to broaden and the exchange process takes place. The linear temperature dependence for the temperature range in which exchange takes place can be seen in Figure 5. In the case of C222 (Figure 3), the exchange process is faster due to the larger cavity of the cryptand. The signals that refer to solvated and complexed Li cation (8.7 and 6.8 ppm, respectively at 223 K) coalescence at ca. 263 K and at high temperature (>313 K) only one sharp signal at 7.7 ppm was observed as a consequence of a very fast exchange process. An accurate temperature dependence for C222 over a large temperature range can be observed in Figure 6.

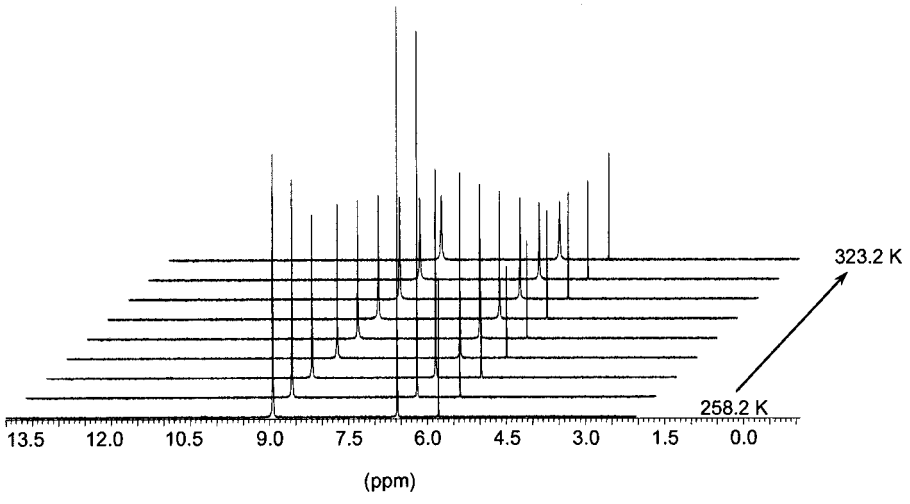

Figure 2. ^7Li NMR spectra recorded as a function of temperature for the mol ratio C221/$LiClO_4$ = 0.5.

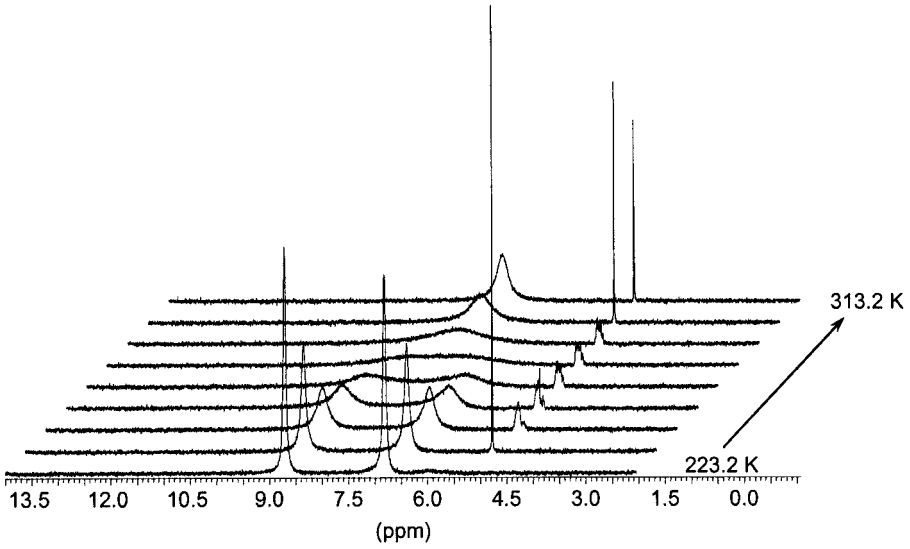

Figure 3. ^{7}Li NMR spectra recorded as a function of temperature for the mol ratio C222/$LiClO_4$ = 0.5.

The rate of the exchange reaction increased not only with increasing cavity size of the cryptand but also with increasing concentration of the chelate, as can be recognized from the shape of the signals at 223 K in Figure 4 and from the values of $k_{obsd.}$ in Table 1 (see Figure 5 and Figure 6). A summary of the all the measured rate constants are given in Tables S1 and S2 (see Supporting Information).

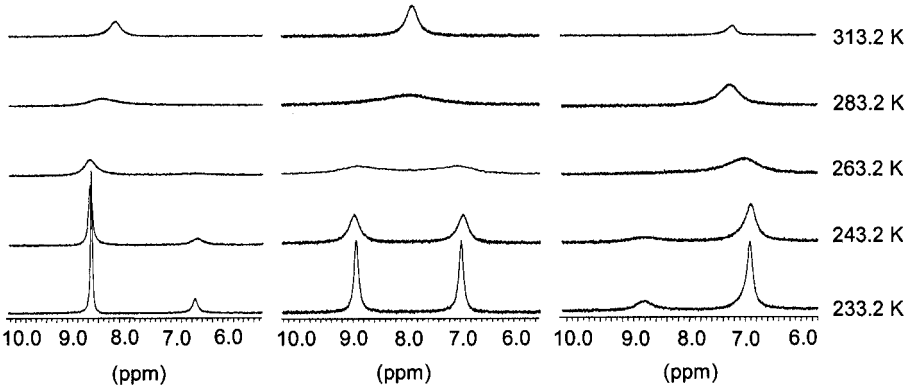

Figure 4. ^{7}Li NMR spectra of C222 and $LiClO_4$ in acetone. Temperature dependence for the sample ratios C222/$LiClO_4$ = 0.25, 0.5 and 0.75, respectively.

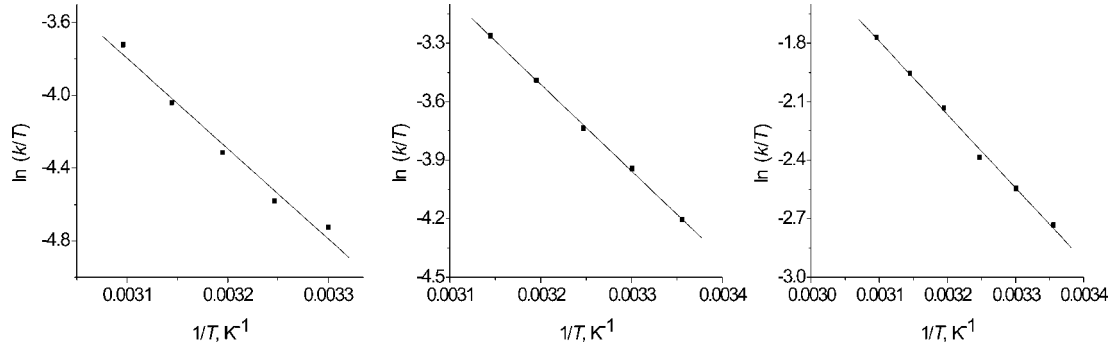

Figure 5. Eyring plots for $k_{obsd.}$ as a function of temperature for C221 in the temperature range in which exchange was observed for the concentration ratios C221/$LiClO_4$ = 0.5, 0.65 and 0.8, respectively.

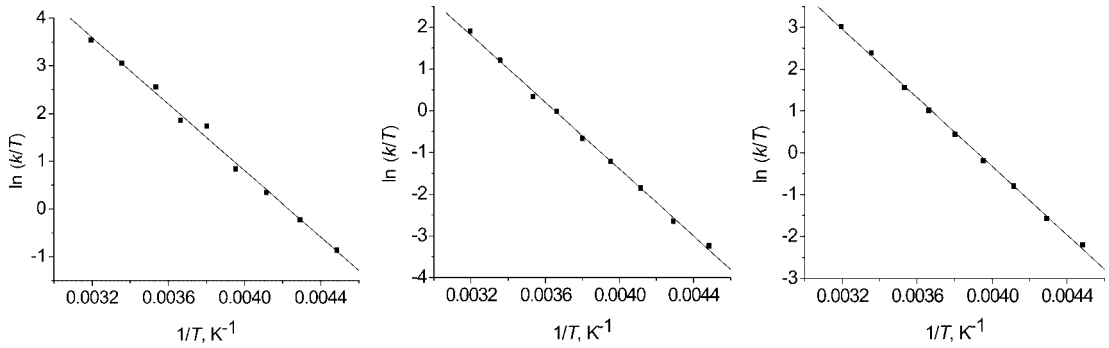

Figure 6. Eyring plots for $k_{obsd.}$ as a function of temperature for C222 for the concentration ratios C222/$LiClO_4$ = 0.25, 0.5 and 0.75, respectively.

Table 1. Values of the observed rate constants ($k_{obsd.}$) and activation parameters calculated from the line-shape analysis for the exchange of Li^+ between solvated and chelated sites at 25 °C.

Molar ratio [L]/[Li^+] C221	$k_{obsd.}^{298}$ [s^{-1}]	$\Delta H^{\#}$ [kJ mol^{-1}]	$\Delta S^{\#}$ [J K^{-1} mol^{-1}]
0.5	2.10 ± 0.04	41 ± 3	–102 ± 12
0.65	4.5 ± 0.1	37 ± 1	–109 ± 3
0.8	19.4 ± 0.8	31 ± 1	–116 ± 4
C222			
0.25	1001 ± 20	33.3 ± 0.5	–76 ± 1
0.5	3263 ± 98	34.1 ± 0.4	–64 ± 1
0.75	6346 ± 254	29 ± 1	–75 ± 2

Suggested Exchange Mechanism

Two mechanisms should be considered for the decomplexation processes of cryptand–alkali-metal complexes: unimolecular (dissociative) and bimolecular (associative) cation exchange. The solvent plays a major role in the unimolecular mechanism and this mechanism is therefore favored in strong donor solvents.[20]

Lincoln et al.[18] investigated many similar systems where the Li^+ cation was exchanged between different cryptands or crown ethers and common solvents. In case of crown ethers and cryptands in non-aqueous solutions, the rates of formation (k_c) for their interaction with alkali-metal cations are generally diffusion controlled and, consequently, the complexation selectivities are governed by the decomplexation rates (k_d). They proposed the operation of a monomolecular mechanism for the decomplexation of Li^+ from the cryptand, notwithstanding the fact that decomplexation is characterized by very negative activation entropies.

According to Popov et al.,[17] there are two possible mechanisms that need to be considered for the exchange of Li^+ cation between the solvated and the complexed sites, viz. bimolecular (associative) (*I*) and unimolecular (dissociative) (back reaction in II) cation exchange processes, where S presents solvent and L the employed chelate.[17,32] (In this description we have added the terms "associative" and "dissociative" because this is implied by the mechanistic interpretation offered by the authors.)

$$*Li(S)^+ + Li(L)^+ \underset{k_{-1}}{\overset{k_1}{\rightleftharpoons}} Li(S)^+ + *Li(L)^+ \quad (I)$$

$$Li(S)^- + L \underset{k_{-2}}{\overset{k_2}{\rightleftharpoons}} Li(L)^+ + S \quad (II)$$

At equilibrium:

$k_1[*Li(S)][Li(L)] = k_{-1}[*Li(L)][Li(S)]$

$k_2[Li(S)][L] = k_{-2}[Li(L)][S]$

Therefore see Equations (1) and (2)

$$-\frac{d}{dt}[Li(S)] = k_{obsd.}[Li(S)] = k_1[Li(S)][Li(L)] + k_{-2}[Li(L)][S] \quad (1)$$

$$k_{obsd.} = k_1[Li(L)] + \frac{k_{-2}[Li(L)][S]}{[Li(S)]} \quad (2)$$

An alternative form of Equation (2) is Equation (3), which was used to fit the data in Figure 7 and Figure 9.

$$\frac{k_{obsd.}}{[Li(S)]} = k_1 + k_{-2}' \cdot \frac{1}{[Li(S)]} \quad (3)$$

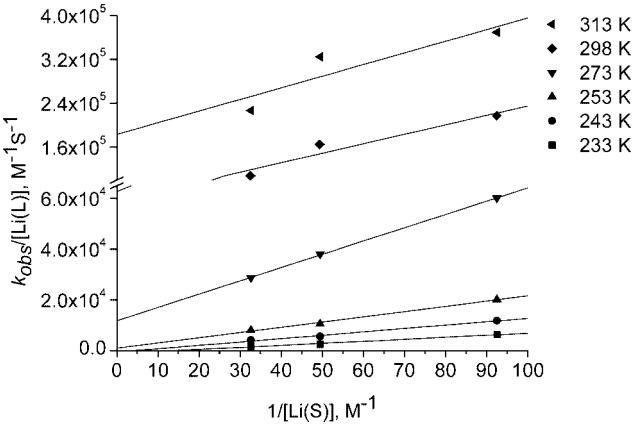

Figure 7. Plots of $k_{obsd.}$/[Li(L)] vs. 1/[Li(S)] for C222 as a function of temperature.

Plots of $k_{obsd.}$/[Li(L)] vs. 1/[Li(S)] were found to be linear with varying slopes ($k_{-2}' = k_{-2}$[S]) and intercepts (k_1) (see Figure 7 and Figure 8). The plots indicate that both path-

ways compete with each other and the competition is controlled by temperature and the nature of the cryptand. In the case of C222 (Figure 7), the plots at low temperature exhibit no meaning intercept, whereas the plots at high temperature exhibit very large intercepts. Thus the contribution from k_1 increases significantly with temperature. In the case of C221 (Figure 8), all the plots exhibit almost no intercept, such that the exchange process is mainly controlled by k_{-2}. The corresponding Eyring plots are shown in Figure 9 and Figure 10, respectively, and the thermal activation parameters are summarized in Table 2.

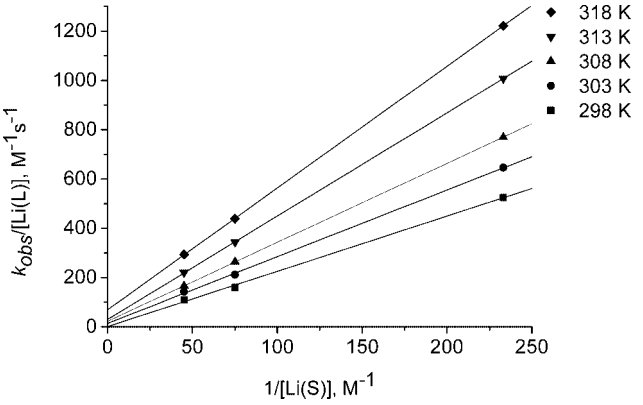

Figure 8. Plots of $k_{obsd.}$/[Li(L)] vs. 1/[Li(S)] for C221 as a function of temperature.

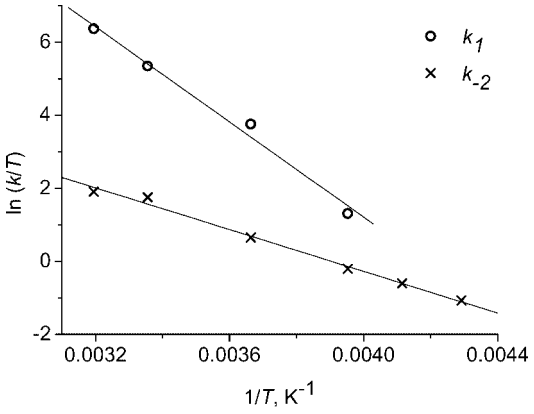

Figure 9. Eyring plots for k_1 and k_{-2} as a function of temperature for C222.

The activation parameters derived from the temperature dependence of k_1 are rather inaccurate due to the large error limits of the intercepts and the reported activation entropy has no mechanistic meaning. On the basis of the values of k_{-2} and the significantly negative activation entropies obtained for this pathway, the activation parameters support an associative type of exchange process. k_{-2} for C222

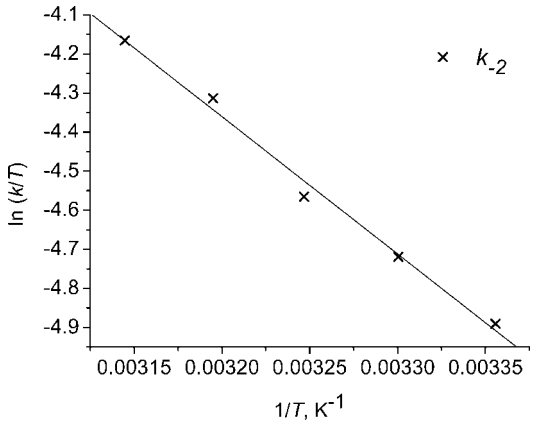

Figure 10. Eyring plot for k_{-2} as a function of temperature for C221.

is almost three orders of magnitude larger than for C221. Furthermore, the activation parameters are very similar to those obtained directly from the values of $k_{obsd.}$ as a function of temperature. This would be in a good agreement with that postulated by Lincoln, who assumed that only the decomplexation process contributes to the observed reaction under the given experimental conditions. The negative activation entropies found for the decomplexation reactions of both C221 and C222 strongly suggest that attack of the solvent on the complexes Li^+ must play an important role in the decomplexation process, i.e. decomplexation follows an associative mechanism (see theoretical calculations).

The reported activation parameters are within the range of those reported by Popov et al. for closely related systems.[17] However, it should be pointed out that they used a different rate law than the one proposed by Shchori et al.[33] and the one used in the present study, which complicates a direct comparison of the reported activation parameters. Nevertheless, although they proposed another mechanism, the values of the activation parameters obtained from their study are very similar to ours, as shown in Table 3.

Table 3. Comparison of activation parameters.

	k_b [s^{-1}]	$\Delta H^{\#}$ [kJ mol^{-1}]	$\Delta S^{\#}$ [J K^{-1} mol^{-1}]
Popov et al.[28]	794 ± 42	20 ± 1	–121 ± 3
This work	1724 ± 484	24 ± 1	–105 ± 4

It is reasonable to expect that solvents such as acetonitrile, acetone and γ-butyrolactone, due to their similar properties as expected from their rather similar Gutmann donor numbers (DN = 14.1, 17.0 and 18.0, respectively,[34]) should coordinate to Li^+ in a similar way and should have a similar influence on the exchange mechanism. This obser-

Table 2. Thermal activation parameters obtained from the values of k_1 and k_{-2} as a function of temperature.

Chelate	k_1^{298} [M^{-1} s^{-1}]	k_{-2}^{298} [s^{-1}]	$\Delta H^{\#}$ [kJ mol^{-1}]	$\Delta S^{\#}$ [J K^{-1} mol^{-1}]
C221		2.24 ± 0.09	29 ± 2	–141 ± 5
C222		(1.7 ± 0.5) × 10^3	24 ± 1	–105 ± 4
C222	(6 ± 3) × 10^4		54 ± 4	+29 ± 15

vation corresponds to that reported by Shamsipur et al.[35] for the exchange of Li^+ between C221 and acetonitrile/nitromethane mixtures. In all solvent mixtures used, Li^+ exchange was found to occur through an associative mechanism, as expected for weakly donor solvents (*DN* = 14.1 and 2.7 for acetonitrile and nitromethane, respectively).

High Pressure ^{7}Li NMR Measurements

Additional mechanistic information on the intimate nature of the exchange mechanism can in principle be obtained from the effect of pressure on the Li^+ exchange process.[36] A systematic pressure dependence study was performed to determine the volume of activation for the Li^+ exchange process for both chelates. Pressure-dependent NMR spectra were recorded for each sample over the pressure range of 0.1 to 150 MPa at 313.2 K. The higher temperature had to be chosen, because in the case of C221 the exchange process hardly occurs at room temperature, whereas in the case of C222 the signals are broad at room temperature due to coalescence and it was difficult to observe line broadening that resulted from increasing pressure. There are two signals to be seen in Figure 11: one for the solvated Li at 8.8 ppm and the one for Li complexed by C221 at 6.5 ppm. It can be observed that there is a very small difference in the shape of the NMR spectra recorded at various pressures. The same effect was observed for the second ligand, C222 (Figure 12), where only one signal appears due to the fast exchange. Its shape almost does not change with the varying pressure for any of the three samples. The rate constants calculated for each pressure were very similar within the experimental error limits and resulted in a practically zero value for $\Delta V^{\#}_{obsd.}$ for both ligands, which points to a concerted interchange type of exchange mechanism.[37] In terms of an interchange mechanism, bond formation and bond cleavage occur in a concerted fashion without the formation of a distinct intermediate of higher or lower coordination number. In addition, decomplexation will be accompanied by charge creation due to the release of Li^+, which in turn will lead to an increase in electrostriction which will offset the intrinsic volume changes.

Theoretical Calculations

For the closely related γ-butyrolactone and Li^+/γ-butyrolactone high level ab initio studies were recently performed by Rey et al.[38] For acetone and Li^+/acetone only Hartree–Fock calculations were performed.[30] In our DFT calculations we found that the Li^+ cation coordinates to the carbonyl oxygen with an almost co-linear configuration relative to the carbon–oxygen bond, as for γ-butyrolactone. This configuration holds for clusters of up to four molecules and also in the solid phase, where a tetrahedral first solvation (coordination) sphere was found (see Table 4).[31]

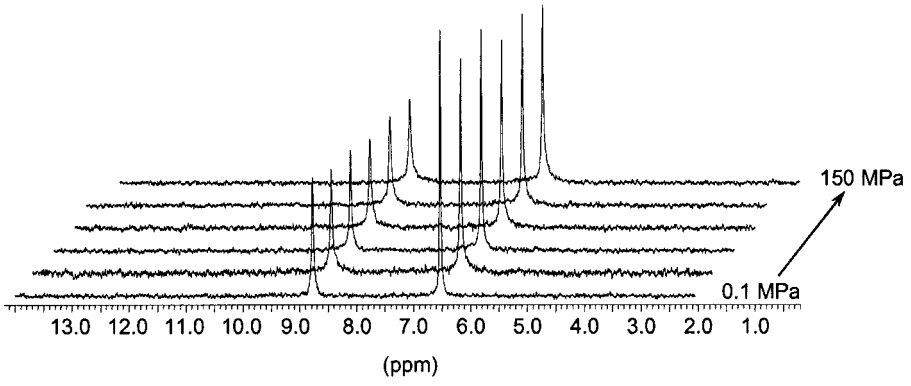

Figure 11. ^{7}Li NMR spectra recorded as a function of pressure at 313.2 K for the mol ratio C221/$LiClO_4$ = 0.5.

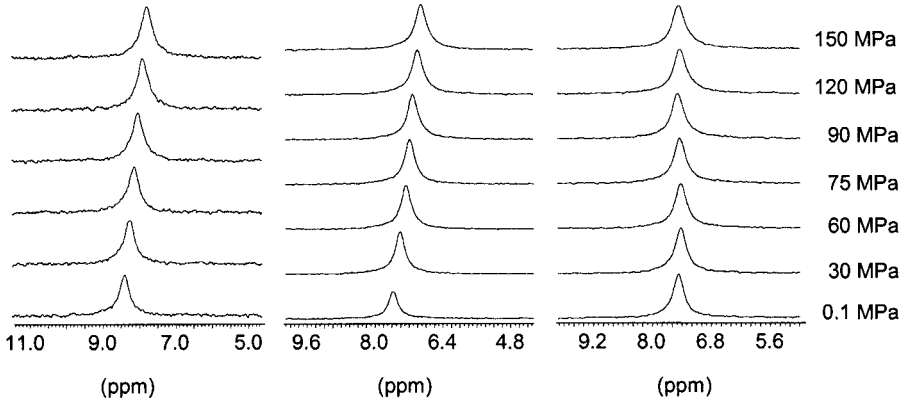

Figure 12. ^{7}Li NMR spectra of C222 and $LiClO_4$ in acetone. Pressure dependence for the sample ratios C222/$LiClO_4$ = 0.25, 0.5, and 0.75, respectively, at 313.2 K.

Table 4. Calculated bond length for Li^+ solvated in acetone.

Bond length [Å]	PG	B3LYP/D95Vp	B3LYP/6-311+G**
$[Li(acetone)]^+$	C_2	1.77	1.75
$[Li(acetone)_2]^+$	D_2	1.81	1.79
$[Li(acetone)_3]^+$	D_3	1.88	1.86
$[Li(acetone)_4]^+$	C_1	1.96 (averaged)	1.96 (averaged)

Experimentally, a decrease in the cavity size of the cryptands hampers the exchange of Li^+ between the cryptand and the solvent. We were able to observe it in the case of γ-butyrolactone and again we can see it in the present case. The improved binding of Li^+ in a smaller cavity is visible from the structure and the following model reaction [Equation (4)] that describes the energy required for the dechelation process. Application of the CPCM solvent model strengthens this trend significantly (see Table 5).

$$[Li \subset Cryptand]^+ + 4\ solvent \rightarrow [Li(solvent)_4]^+ + Cryptand \quad (4)$$

Table 5. Dechelation energy, $E_{dechelation}$, for the reaction outlined in Equation (4).[a]

Acetone	C222	C221	C211
$E_{dechelation}$ (DFT) [kcal/mol]	–8.6	+2.0	+3.0
$E_{dechelation}$ (CPCM) [kcal/mol]	+5.4	+13.6	+20.4
γ-Butyrolactone	C222	C221	C211
$E_{dechelation}$ (DFT) [kcal/mol][21]	–16.8	–11.6	–5.3

[a] DFT: RB3LYP/D95Vp, CPCM: RB3LYP(CPCM)/D95Vp//RB3LYP/D95Vp.

In agreement with previous studies by Wipff et al.,[3] we also found only a limited flexibility for the investigated cryptands in our DFT calculations, therefore all cryptands were calculated within the highest possible symmetry (Table 5). We recently demonstrated that reaction (4) is a valuable tool to determine ion selectivity as a function of the ionic radii[39] and to examine cavity size of the cryptands as a variable.[21,40]

In agreement with the experimental kinetic data, the smaller cryptand binds Li^+ better and slows down its exchange rate (Table 2). On comparing the calculated Li–O and Li–N bond lengths of the three structures with the bond length in $[Li(OH_2)_4]^+$ and $[Li(NH_3)_4]^+$, the trend can easily be understood (see Table 6 and Figure 11). In C222, Li^+ is four-fold weakly coordinated in a trigonal-pyramidal shape by one Li–N and three Li–O interactions all clearly elongated (0.2 and 0.1 Å, respectively). The Li^+ cation in C221 is five-fold coordinated (distorted trigonal-bipyramidal structure) by one nitrogen and four oxygen bonds all extended by around 0.15 Å. The coordinating bonds in $[Li \subset C211]^+$ are even more extended, but the Li–O bonds form a somewhat distorted tetrahedral coordination sphere for the lithium monocation, while the stronger elongated Li–N bonds form a kind of second coordination sphere. Therefore, the lithium ion can formally adopt a six-coordinate state, which strongly supports the proposed associative character of the decomplexation process that involves binding of external solvent molecules as suggested by the very negative activation entropies. A comparison of the calculated and X-ray bond lengths shows a good agreement. A comparison between the calculated data for γ-butyrolactone and acetone shows the same trend for both solvents. Li^+ is better coordinated in the smaller cavities of the smaller cryptands, as expected.

To draw a conclusion on solvation abilities from a direct comparison of the dechelating energies in acetone and γ-butyrolactone, is risky. The calculated dechelating energies can not be considered as a proof of the rule of Madrakian et al., that there is an inverse relationship between the stability of the complexes and the solvating ability of the solvent.[31] The different values can be attributed to the different number of non-hydrogen atoms in both solvents. Acetone has only four non-hydrogen atoms, while γ-butyrolactone has six and can therefore stabilize charge much better.

Conclusions

It can be concluded from the results of the present study that for the Li^+ exchange process between C222, C221 and acetone as solvent, two pathways, viz. bimolecular (associative) and unimolecular (dissociative) compete with each other. The pressure dependence of the exchange process suggests the operation of a pure interchange mechanism, whereas the negative activation entropy values favor an associative interchange process for the decomplexation reaction. The basic idea of an interchange process involves concerted bond formation and bond cleavage, which is in agreement with the consideration that acetone is a rather weak

Table 6. Calculated (RB3LYP/D95Vp) and X-ray bond lengths (in Å).

d [Å]	C222	C221	C211	$[Li(OH_2)_4]^+$	$[Li(acetone)_4]^+$	$[Li(NH_3)_4]^+$
Li–O	2.14	2.06, 2.08, 2.10	2.14, 2.11	1.95	1.96	–
Li–N	2.22	2.28	2.38	–	–	2.13
PG	C_3	C_1	C_2	T	C_1	C_1
X-ray		[41]	[42]	[43]	[44]	[45]
Li–O	–	1.99 2.06 2.10	2.17 2.08	1.96	1.94, 1.91, 1.93, 1.95	–
Li–N	–	2.40 2.44	2.29	–	–	2.08

donor. The results are in good agreement with that expected on the basis of a systematic comparison with data reported in the literature for solvents of similar donor strength.

Experimental Section

General Procedures: The preparation of test solutions was carried out under Ar or N_2 using standard Schlenk techniques, under an Ar in a glove box, or under vacuum. Lithium perchlorate (Aldrich, battery grade) was vacuum-dried at 120 °C for 48 h and then stored under dry nitrogen. The cryptands C222 (purchased from Fluka), C221 and C211 (purchased from Aldrich) were dried under vacuum for 48 h and stored under dry nitrogen. Acetone (Acros, extra dry, water < 50 ppm) was used as received. Solutions of $LiClO_4$, C222, C221 and C211 in acetone were prepared under dry nitrogen. For the ^{7}Li NMR measurements the solutions were sealed in 5-mm NMR tubes under Ar. In order to study the kinetics of the exchange of Li^+ between C222 and C221 and acetone as solvent, three solutions of different concentration ratio were prepared for each system. The concentration of lithium perchlorate in each solution was kept constant at 0.04 M, whereas the concentration of ligand was varied between 0.01 M and 0.032 M. In this way the measurements were always performed in the presence of an excess of Li^+.

^{7}Li NMR Spectroscopy: Variable-temperature and variable-pressure Fourier transform ^{7}Li NMR spectra were recorded at a frequency of 155 MHz with a Bruker Avance DRX 400WB spectrometer equipped with a superconducting BC-94/89 magnet system. Spinning tubes (5 mm) were used with a 1-mm o.d. melting point capillary inserted coaxially in the spinning tube and filled with an external reference solution (1 M $LiClO_4$ in acetonitrile). The temperature dependence measurements were performed over a wide as possible temperature range for each system. We did not use a temperature calibration by insertion of a capillary filled with methanol (low temperature calibration) or ethylene glycol (high temperature calibration) into the sample tube, as the corresponding signals of these solvents would disturb the NMR spectra in the region of interest. In such a case a temperature-calibrated NMR probe has to be used in order to determine the temperature of the sample accurately.

Methanol was used for the low-temperature calibration of the NMR probe, whereas ethylene glycol was used for high-temperature calibration. The actual sample temperature can be calculated from the chemical shift differences. If there is any difference between the sample temperature and the temperature detected by the thermocouple of the probe, the probe can be calibrated by using standard Bruker Topspin software.

A homemade high-pressure probe described in the literature[46] was used for the variable-pressure experiments which were conducted at a selected temperature and at ambient, 30, 60, 75, 90, 120 and

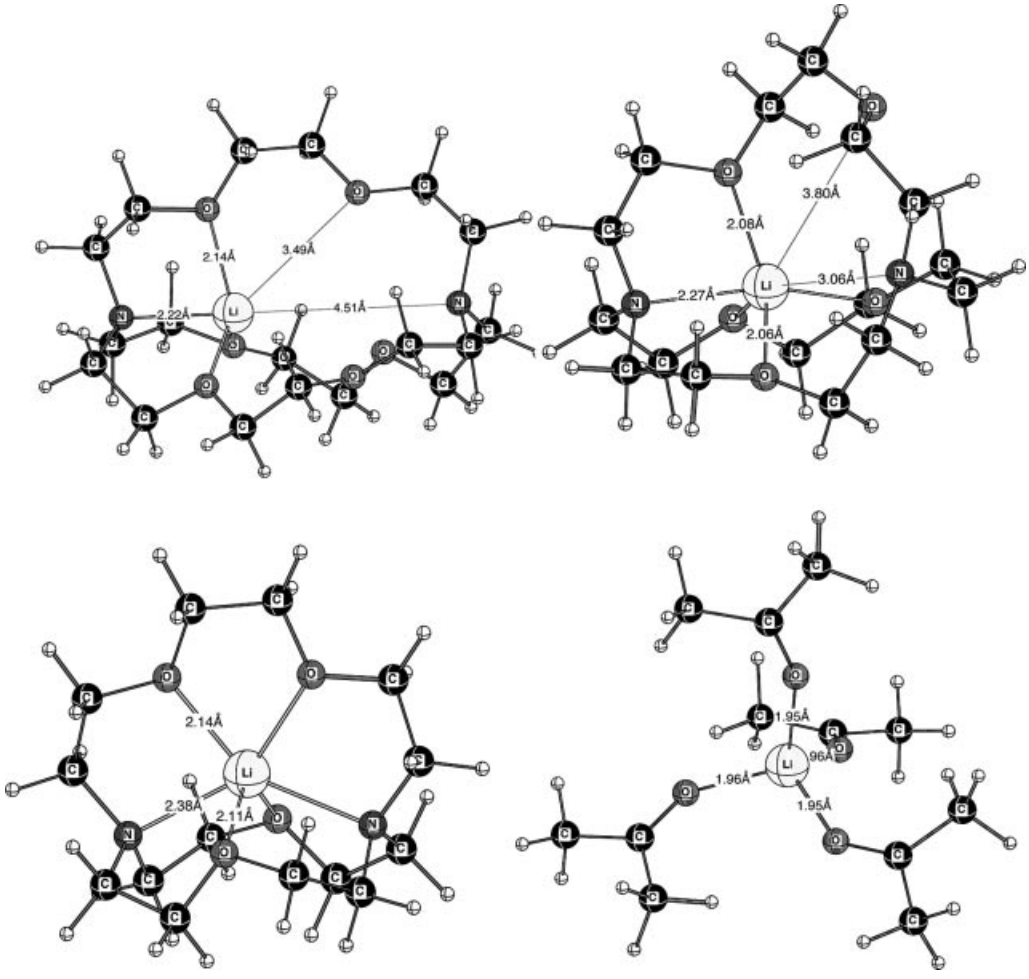

Figure 13. Optimized structures for $[Li \subset C222]^+$, $[Li \subset C221]^+$, $[Li \subset C211]^+$ and $[Li(acetone)_4]^+$.

150 MPa pressure. A standard 5-mm NMR tube cut to a length of 45 mm was used for the sample solution. The high-pressure NMR tube was sealed with a MACOR plug and an O-ring made of VITON. The plug and O-ring were shown to be stable in the employed solvent. The pressure was transmitted by the movable MACOR piston to the sample, and the temperature of the sample was controlled with a Pt-100 resistor. The probe itself was externally heated with a thermostatted circulating fluid that was pumped through a double helix that was cut into the outer surface of the autoclave. Because the sample is embedded in the high-pressure transmitting fluid that serves as a thermostating bath, a reliable temperature setting is guaranteed.

For a typical kinetic run, 0.8 mL of solution was transferred under Ar to a Wilmad screw-cap NMR tube equipped with a poly(tetrafluoroethylene) septum. All test samples were prepared in the same way.

Programs: The line widths of the NMR signals were obtained by fitting Lorentzian functions to the experimental spectra using the NMRICMA 2.7 program[47] for Matlab.[48] The adjustable parameters were the resonance frequency, intensity, line width and baseline. Complete line-shape analysis based on the Kubo–Sack formalism using modified Bloch equations[49] was also performed with NMRICMA 2.7 to extract rate constants from experimental spectra. The temperature and pressure dependent ^{7}Li line widths and chemical shifts employed in the line shape analysis were extrapolated from low temperatures where no exchange-induced modification occurred.

Quantum Chemical Calculations: All structures were optimized with the B3LYP[50] and the basis set D95Vp,[51] or with 6-311+G** with no constrains other than symmetry, and confirmed to be minima by computation of vibrational frequencies. Relative energies were corrected for zero point vibrational energy differences (Figure 13). The D95V basis set, augmented with polarisation functions (D95Vp), was used.[52] If not otherwise mentioned, calculations were done without a solvent model. The influence of bulk solvent was probed using the CPCM[53] formalism and water as solvent, i.e., B3LYP(CPCM)/D95Vp//B3LYP/D95Vp. The Gaussian 03 suite of programs was used throughout.[54]

Supporting Information (see also the footnote on the first page of this article): Two tables with values of the observed rate constants (k_{obs}) calculated from the line shape analysis for the exchange of Li^+ between solvated and chelated sites for two cryptands.

Acknowledgments

This work was supported by the European Commission Training and Mobility of Researchers Network (HPRN-CT-2000-19, "Solvation Dynamics and Ionic Mobility in Conventional and Polymer Solvents") and the Deutsche Forschungsgemeinschaft (SFB 583 on Redox-active Metal Complexes). We would like to thank Dr. Lothar Helm (EPFL Lausanne) for introducing E. P. to the software NMRICMA 2.7, Dr. Nico van Eikema Hommes for helpful discussions, Michael Galle for preliminary calculations, Prof. Tim Clark for hosting this work in the CCC and the Regionales Rechenzentrum Erlangen (RRZE) for a generous allotment of computer time.

[1] a) B. Dietrich, J. M. Lehn, J. P. Sauvage, *Tetrahedron Lett.* **1969**, *34*, 2889–2892; b) B. Dietrich, J. M. Lehn, J. P. Sauvage, *Tetrahedron Lett.* **1969**, *34*, 2885–2888.

[2] a) J. M. Lehn, *Acc. Chem. Res.* **1978**, *11*, 49–57; b) J. M. Lehn, *Angew. Chem.* **1988**, *100*, 91–116.

[3] G. Wipff, J. M. Wurtz, *New J. Chem.* **1989**, *13*, 807–820.

[4] X. X. Zhang, R. M. Izatt, K. E. Krakowiak, J. S. Bradshaw, *Inorg. Chim. Acta* **1997**, *254*, 43–47.

[5] J. M. Lehn, F. Montavon, *Helv. Chim. Acta* **1976**, *59*, 1566–1583.

[6] a) R. Puchta, V. Seitz, N. J. R. van Eikema Hommes, R. W. Saalfrank, *J. Mol. Model.* **2000**, *6*, 126–132; b) R. W. Saalfrank, A. Dresel, V. Seitz, S. Trummer, F. Hampel, M. Teichert, D. Stalke, C. Stadler, J. Daub, V. Schunemann, A. X. Trautwein, *Chem. Eur. J.* **1997**, *3*, 2058–2062; c) R. W. Saalfrank, V. Seitz, D. L. Caulder, K. N. Raymond, M. Teichert, D. Stalke, *Eur. J. Inorg. Chem.* **1998**, *9*, 1313–1317; d) R. W. Saalfrank, V. Seitz, F. W. Heinemann, C. Gobel, R. Herbst-Irmer, *J. Chem. Soc., Dalton Trans.* **2001**, *5*, 599–603.

[7] B. Dietrich, J. P. Kintzinger, J. M. Lehn, B. Metz, A. Zahidi, *J. Phys. Chem.* **1987**, *91*, 6600–6606.

[8] L. F. Lindoy, *The Chemistry of Macrocyclic Ligand Complexes*, Cambridge University Press, Cambridge, **1992**, p. 269.

[9] a) M. Farahbakhsh, H. Schmidt, D. Rehder, *Chem. Ber./Recueil* **1997**, *130*, 1123–1127; b) C. E. Housecroft, *Cluster Compounds of Main Group Elements*, VCH, Weinheim, Germany, **1996**, p. 94; c) M. Kirch, J. M. Lehn, *Angew. Chem.* **1975**, *87*, 542–543; d) J. M. Lehn, F. Montavon, *Helv. Chim. Acta* **1978**, *61*, 67–82; e) W. E. Morf, W. Simon, *Helv. Chim. Acta* **1971**, *54*, 2683–2704; f) M. J. Pregel, E. Buncel, *J. Am. Chem. Soc.* **1993**, *115*, 10–14; g) W. Simon, W. E. Morf, P. C. Meier, *Struct. Bond.* **1973**, *16*, 113–160.

[10] J. M. Lehn, J. P. Sauvage, *J. Chem. Soc., Chem. Commun.* **1971**, *9*, 440–441.

[11] K. Severin, *Coord. Chem. Rev.* **2003**, *245*, 3–10.

[12] R. H. Huang, M. J. Wagner, D. J. Gilbert, K. A. Reidy-Cedergren, D. L. Ward, M. K. Faber, J. L. Dye, *J. Am. Chem. Soc.* **1997**, *119*, 3765–3772.

[13] J. M. Lehn, J. P. Sauvage, *J. Am. Chem. Soc.* **1975**, *97*, 6700–6707.

[14] G. Wipff, P. Kollman, *Nouv. J. Chim.* **1985**, *9*, 457–465.

[15] B. G. Cox, J. Garcia-Rosas, H. Schneider, *J. Am. Chem. Soc.* **1981**, *103*, 1054–1059.

[16] R. R. Rhinebarger, A. I. Popov, *Polyhedron* **1988**, *7*, 1341–1347; A. J. Smetana, A. I. Popov, *J. Solution Chem.* **1980**, *9*, 183–196.

[17] M. Shamsipur, A. I. Popov, *J. Phys. Chem.* **1986**, *90*, 5997–5999.

[18] a) A. Abou-Hamdan, S. F. Lincoln, *Inorg. Chem.* **1991**, *30*, 462–466; b) P. Clarke, J. M. Gulbis, S. F. Lincoln, E. R. T. Tiekink, *Inorg. Chem.* **1992**, *31*, 3398–3404; c) P. Clarke, S. F. Lincoln, E. R. T. Tiekink, *Inorg. Chem.* **1991**, *30*, 2747–2751; d) S. F. Lincoln, A. Abou-Hamdan, *Inorg. Chem.* **1990**, *29*, 3584–3589; e) S. F. Lincoln, T. Rodopoulos, *Inorg. Chim. Acta* **1991**, *190*, 223–229; f) S. F. Lincoln, T. Rodopoulos, *Inorg. Chim. Acta* **1993**, *205*, 23–30; g) S. F. Lincoln, A. K. W. Stephens, *Inorg. Chem.* **1991**, *30*, 3529–3534; h) A. K. W. Stephens, R. S. Dhillon, S. E. Madbak, S. L. Whitbread, S. F. Lincoln, *Inorg. Chem.* **1996**, *35*, 2019–2024.

[19] a) R. M. Izatt, J. S. Bradshaw, S. A. Nielsen, J. D. Lamb, J. J. Christensen, D. Sen, *Chem. Rev.* **1985**, *85*, 271–339; b) R. M. Izatt, J. S. Bradshaw, K. Pawlak, R. L. Bruening, B. J. Tarbet, *Chem. Rev.* **1992**, *92*, 1261–1354; c) R. M. Izatt, K. Pawlak, J. S. Bradshaw, R. L. Bruening, *Chem. Rev.* **1995**, *95*, 2529–2586.

[20] R. M. Izatt, K. Pawlak, J. S. Bradshaw, R. L. Bruening, *Chem. Rev.* **1991**, *91*, 1721–1785.

[21] E. Pasgreta, R. Puchta, M. Galle, N. van Eikema Hommes, R. van Eldik, *J. Inclusion Phenom. Macrocyclic Chem.* **2007**, *58*, 81–88.

[22] a) K. Sonoda, M. Deguchi, H. Koshina, M. Armand, C. Michot, M. Gauthier, *Proc. Electrochem. Soc.* **2003**, 512–517; b) N. Takami, M. Sekino, T. Ohsaki, M. Kanda, M. Yamamoto, *J. Power Sources* **2001**, *97–98*, 677–680.

[23] *Spec. Issue*: S. T. Handy, P. A. Grieco, C. Mineur, L. Ghosez, *Synlett* **1995**, 565–567.

[24] W. J. Kinart, E. Sniec, I. Tylak, C. M. Kinart, *Phys. Chem. Liq.* **2000**, *38*, 193–201.
[25] a) J. Barthel, R. Buchner, E. Wismeth, *J. Solution Chem.* **2000**, *29*, 937–954; b) J. Barthel, H. J. Gores, R. Neueder, A. Schmid, *Pure Appl. Chem.* **1999**, *71*, 1705–1716; c) F. Croce, A. D'Aprano, C. Nanjundiah, V. R. Koch, C. W. Walker, M. Salomon, *J. Electrochem. Soc.* **1996**, *143*, 154–159; d) K. Matsubara, R. Kaneuchi, N. Maekita, *J. Chem. Soc., Faraday Trans.* **1998**, *94*, 3601–3605; e) J. M. Alia, H. G. M. Edwards, *Vib. Spectrosc.* **2000**, *24*, 185–200; f) G. Kumar, Janakiraman, N. Namboodiri, Gangadharan, Saminathan, Kanagaraj, N. Sharief, *J. Chem. Eng. Data* **1991**, *36*, 467–470; g) R. Puchta, M. Galle, N. van Eikema Hommes, E. Pasgreta, R. van Eldik, *Inorg. Chem.* **2004**, *43*, 8227–8229; h) D. Spångberg, K. Hermansson, *Chem. Phys.* **2004**, *300*, 165–176.
[26] a) S. Himeno, M. Takamoto, T. Ueda, R. Santo, A. Ichimura, *Electroanalysis* **2004**, *16*, 656–660; b) M. Hojo, H. Hasegawa, N. Hiura, *J. Phys. Chem.* **1996**, *100*, 891–896.
[27] E. Karkhaneei, M. H. Zebrajadian, M. Shamsipur, *J. Inclusion Phenom. Macrocyclic Chem.* **2001**, *40*, 309–312.
[28] a) J. M. Alia, Y. Diaz de Mera, H. G. M. Edwards, F. J. Garcia, E. E. Lawson, *J. Mol. Struct.* **1997**, *408–409*, 439–450; b) M. Chabanel, D. Legoff, K. Touaj, *J. Chem. Soc., Faraday Trans.* **1996**, *92*, 4199–4205; c) M. Hojo, H. Hasegawa, Y. Morimoto, *Anal. Sci.* **1996**, *12*, 521–524; d) J. Barthel, R. Neueder, H. Poepke, H. Wittmann, *J. Solution Chem.* **1999**, *28*, 489–503; e) V. D. Kiselev, E. A. Kashaeva, N. A. Luzanova, A. I. Konovalov, *Thermochim. Acta* **1997**, *303*, 225–228; f) Y. Kameda, N. Kudoh, S. Suzuki, T. Usuki, O. Uemura, *Bull. Chem. Soc. Jpn.* **2001**, *74*, 1009–1014.
[29] R. J. Blint, *J. Electrochem. Soc.* **1995**, *142*, 696–702.
[30] R. L. Jarek, T. D. Miles, M. L. Trester, S. C. Denson, S. K. Shin, *J. Phys. Chem. A* **2000**, *104*, 2230–2237.
[31] T. Madrakian, A. Afkhami, J. Ghasemi, M. Shamsipur, *Polyhedron* **1996**, *15*, 3647–3652.
[32] E. Shchori, J. Jagur-Grodzinski, M. Shporer, *J. Am. Chem. Soc.* **1973**, *95*, 3842–3846.
[33] E. Shchori, J. Jagur-Grodzinski, Z. Luz, M. Shporer, *J. Am. Chem. Soc.* **1971**, *93*, 7133–7138.
[34] Y. Marcus, *Chem. Soc. Rev.* **1993**, *22*, 409–416.
[35] M. Shamsipur, E. Karkhaneei, A. Afkhami, *J. Coord. Chem.* **1998**, *44*, 23–32.
[36] a) A. V. Davis, D. Fiedler, G. Seeber, A. Zahl, R. van Eldik, K. N. Raymond, *J. Am. Chem. Soc.* **2006**, *128*, 1324–1333; b) R. van Eldik, C. D. Hubbard, *Chemistry at Extreme Conditions*, Elsevier, Amsterdam, **2005**, p. 109–164; c) M. Wolak, R. van Eldik, *J. Am. Chem. Soc.* **2005**, *127*, 13312–13315; d) A. Zahl, R. van Eldik, M. Matsumoto, T. W. Swaddle, *Inorg. Chem.* **2003**, *42*, 3718–3722; e) J. R. Rustad, A. G. Stack, *J. Am. Chem. Soc.* **2006**, *128*, 14778–14779.
[37] L. Helm, A. E. Merbach, *Chem. Rev.* **2005**, *105*, 1923–1959.
[38] M. Masia, R. Rey, *J. Phys. Chem. B* **2004**, *108*, 17992–18002.
[39] M. Galle, R. Puchta, N. J. R. van Eikema Hommes, R. van Eldik, *Z. Phys. Chem.* **2006**, *220*, 511–523.
[40] R. Puchta, R. van Eldik, *Eur. J. Inorg. Chem.* **2007**, 1120–1127.
[41] S. Choua, H. Sidorenkova, T. Berclaz, M. Geoffroy, P. Rosa, N. Mezailles, L. Ricard, F. Mathey, P. Le Floch, *J. Am. Chem. Soc.* **2000**, *122*, 12227–12234.
[42] D. Moras, R. Weiss, *Acta Crystallogr., Sect. B: Struct. Sci.* **1973**, *29*, 400–403.
[43] W. Meske, D. Babel, *Z. Anorg. Allg. Chem.* **1998**, *624*, 1751–1755.
[44] F. A. Cotton, L. M. Daniels, C. A. Murillo, H. C. Zhou, *Inorg. Chim. Acta* **2000**, *300–302*, 319–327.
[45] N. Scotti, U. Zachwieja, H. Jacobs, *Z. Anorg. Allg. Chem.* **1997**, *623*, 1503–1505.
[46] A. Zahl, A. Neubrand, S. Aygen, R. van Eldik, *Rev. Sci. Instrum.* **1994**, *65*, 882–886.
[47] L. Helm, A. Borel *NMRICMA 2.7*, University of Lusanne, **2000**.
[48] *Matlab*, version 5.3.1., Mathworks Inc., **1999**.
[49] J. A. Pople, W. G. Schneider, H. J. Bernstein, *High-Resolution Nuclear Magnetic Resonance*, McGrow-Hill Book Co., New York, **1959**, p. 513.
[50] a) A. D. Becke, *J. Chem. Phys.* **1993**, *98*, 5648–5652; b) C. Lee, W. Yang, R. G. Parr, *Phys. Rev. B: Condens. Matter* **1988**, *37*, 785–789; c) P. J. Stephens, F. J. Devlin, C. F. Chabalowski, M. J. Frisch, *J. Phys. Chem.* **1994**, *98*, 11623–11627.
[51] a) T. H. Dunning Jr, P. J. Hay, *Modern Theoretical Chemistry*, Plenum, New York, **1976**, vol. 3, p. 1–28; b) S. Huzinaga, J. Andzelm, M. Klobukowski, E. Radzio-Andzelm, Y. Sakai, H. Tatewaki, *Gaussian basis sets for molecular calculations*, Elsevier, Amsterdam, **1984**.
[52] a) The performance of the computational level employed in this study is well documented, see for example: M. Galle, R. Puchta, N. van Eikema Hommes, R. van Eldik, *Z. Phys. Chem.* **2006**, *220*, 511–523; R. Puchta, N. J. R. van Eikema Hommes, R. Meier, R. van Eldik, *Dalton Trans.* **2006**, *28*, 3392–3395; S. Klaus, H. Neumann, H. Jiao, A. Jacobi von Wangelin, D. Goerdes, D. Struebing, S. Huebner, M. Hateley, C. Weckbecker, K. Huthmacher, T. Riermeier, M. Beller, *J. Organomet. Chem.* **2004**, *689*, 3685–3700; R. W. Saalfrank, C. Deutscher, H. Maid, A. M. Ako, S. Sperner, T. Nakajima, W. Bauer, F. Hampel, B. A. Hess, N. J. R. van Eikema Hommes, R. Puchta, F. W. Heinemann, *Chem. Eur. J.* **2004**, *10*, 1899–1905; A. Scheurer, H. Maid, F. Hampel, R. W. Saalfrank, L. Toupet, P. Mosset, R. Puchta, N. J. R. van Eikema Hommes, *Eur. J. Org. Chem.* **2005**, *12*, 2566–2574; C. F. Weber, R. Puchta, N. J. R. van Eikema Hommes, P. Wasserscheid, R. van Eldik, *Angew. Chem.* **2005**, *117*, 6187–6192; C. F. Weber, R. Puchta, N. J. R. van Eikema Hommes, P. Wasserscheid, R. van Eldik, *Angew. Chem. Int. Ed. Engl.* **2005**, *44*, 6033–6038; b) R. Puchta, M. Galle, N. J. R. van Eikema Hommes, *Z. Naturforsch., Teil B* **2006**, *61*, 1327–1334.
[53] a) V. Barone, M. Cossi, *J. Phys. Chem. A* **1998**, *102*, 1995–2001; b) M. Cossi, N. Rega, G. Scalmani, V. Barone, *J. Comput. Chem.* **2003**, *24*, 669–681.
[54] M. J. Frisch, G. W. Trucks, H. B. Schlegel, G. E. Scuseria, M. A. Robb, J. R. Cheeseman, J. A. Montgomery Jr, T. Vreven, K. N. Kudin, J. C. Burant, J. M. Millam, S. S. Iyengar, J. Tomasi, V. Barone, B. Mennucci, M. Cossi, G. Scalmani, N. Rega, G. A. Petersson, H. Nakatsuji, M. Hada, M. Ehara, K. Toyota, R. Fukuda, J. Hasegawa, M. Ishida, T. Nakajima, Y. Honda, O. Kitao, H. Nakai, M. Klene, X. Li, J. E. Knox, H. P. Hratchian, J. B. Cross, V. Bakken, C. Adamo, J. Jaramillo, R. Gomperts, R. E. Stratmann, O. Yazyev, A. J. Austin, R. Cammi, C. Pomelli, J. W. Ochterski, P. Y. Ayala, K. Morokuma, G. A. Voth, P. Salvador, J. J. Dannenberg, V. G. Zakrzewski, S. Dapprich, A. D. Daniels, M. C. Strain, O. Farkas, D. K. Malick, A. D. Rabuck, K. Raghavachari, J. B. Foresman, J. V. Ortiz, Q. Cui, A. G. Baboul, S. Clifford, J. Cioslowski, B. B. Stefanov, G. Liu, A. Liashenko, P. Piskorz, I. Komaromi, R. L. Martin, D. J. Fox, T. Keith, M. A. Al-Laham, C. Y. Peng, A. Nanayakkara, M. Challacombe, P. M. W. Gill, B. Johnson, W. Chen, M. W. Wong, C. Gonzalez, J. A. Pople, *Gaussian 03, Revision B.03, Gaussian Inc.*, Wallingford, CT, **2004**.

Received: December 11, 2006
Published Online: May 10, 2007

